Comparison of Sorbents and Isotherm Models for NH_3-Gas Separation by Adsorption

Jarkko Helminen, Joni Helenius, and Erkki Paatero
Laboratory of Industrial Chemistry, Lappeenranta University of Technology, FIN-53851 Lappeenranta, Finland

Ilkka Turunen
Laboratory of Process Systems Engineering, Lappeenranta University of Technology, FIN-53851 Lappeenranta, Finland

Adsorption equilibrium isotherms of ammonia gas were measured at temperatures between 298 and 393 K on 13X zeolite, 4A zeolite, alumina, silica gel, and activated carbon. The applicability of these sorbents to ammonia gas separation was compared based on equilibrium data. In the pressure range of 1 to 100 kPa activated carbon has its highest working capacity ($5.5\ mmol \cdot g^{-1}$) at 298 K, and the working capacity drops rapidly with temperature, reaching its lowest point at 393 K. The two zeolites provide almost the same working capacity, $3.0-3.5\ mmol \cdot g^{-1}$, over the entire temperature range. Silica gel and alumina showed low working capacities. The experimental equilibrium data were fitted to 16 different isotherm models, with accuracy and reliability statistically evaluated. The Langmuir–Freundlich model with the van't Hoff equation for the equilibrium constant and with a thermal expansion equation for the saturation sorbate concentration provided the most accurate fit for the 13X and 4A zeolites. This model was also very accurate for the alumina and silica gel data, even though the Dubinin– Astakhov model gave slightly higher predictions. The Henry and vacancy solution models provided the best fit for activated carbon.

Introduction

Ammonia is widely used in the chemical industry as a raw material for the synthesis of various chemicals, including fertilizers, nitric acid, urea, melamine, explosives, dyes, and plastics. Generally, chemical processes utilizing ammonia produce ammonia-containing gas mixtures, and ammonia-gas separation is highly necessary and desirable. In addition to these processes, the ammonia manufacturing process itself (Haber–Bosch) also produces dilute ammonia-gas streams that require separation and recovery.

Ammonia-gas separation is conventionally accomplished by cryogenic distillation. The method is economical only on a very large scale, since both the investment and operating costs are high. On small and intermediate scales, ammonia can be separated with gas absorbers. This technique has some drawbacks, such as difficult operability, high investment costs, and the loss of absorbing solutions due to degradation (Lavie, 1985; Hirai et al., 1987; Knaebel, 1998).

Ammonia-gas separation by adsorption and recovery for reuse is well known, but the process has not been applied extensively. The problems with separation are related to the selectivity, capacity, and regenerability of the sorbents. Regenerability, in particular, is an important property for any industrial application, since ammonia is adsorbed very strongly on many sorbents. Most applications are related to the separation of ammonia from the gas streams in the ammonia manufacturing process, where zeolite, alumina, silica gel, and activated carbon can be used as a sorbent (Isalski, 1981; Lavie, 1985; Knaebel, 1998). However, there is no available information on which sorbent works best. In these streams, compounds other than ammonia (such as hydrogen, nitrogen, argon, and methane) can be regarded as nonadsorbing; therefore, the selective separation can be achieved. In general, the separation of ammonia by adsorption is easiest to accomplish in the absence of water.

Correspondence concerning this article should be addressed to J. Helminen.

The sorbent properties can be assessed on the basis of adsorption equilibrium isotherms (Ruthven, 1984; Yang, 1987; Ruthven et al., 1994; Knaebel, 1995). However, reliable and technically useful adsorption equilibrium data for ammonia gas on different sorbent types are available only to a limited extent (Valenzuela and Mayers, 1989; Spindler et al., 1990; Chiachotni et al., 1991). The first task in the present study therefore was to measure ammonia adsorption isotherms on zeolite, alumina, silica gel, and activated carbon sorbents over a wide temperature and pressure range, and to find out the potential applicability of these sorbents in a pressure swing adsorption (PSA) process. Especially, the measurements were directed to the separation of ammonia from dry gas streams, which are formed in the production of organic nitrogen compounds, such as urea and melamine. The selection of particular sorbents was based on the preliminary experiments where the isotherms of different zeolites, aluminas, silica gels, and activated carbons were measured. The selected sorbents showed the most promising properties within each material group.

The second task of this work was the modeling of adsorption equilibrium data and a comparison of isotherm models that could reliably predict ammonia equilibria at low and high temperatures for process design purposes. At present, only a few comparisons of the ammonia isotherm models have been published (Kuo et al., 1985; Shiralkar and Kulkarni, 1985; Chiachotni et al., 1991). Kuo et al., for example, fitted the ammonia equilibrium data for silica gel to the Langmuir and potential theory isotherm models. These data, covering a temperature range of 298–333 K and a pressure range of 2.7–27 kPa, were based on breakthrough experiments. The authors found that the potential theory model correlates considerably better with the measured data than with the Langmuir model, but a detailed calculation of the potential theory parameters, such as sorbate volumes and ammonia vapor pressures, was not given. In general, the temperature dependence of many adsorption isotherm models is not well defined. An industrially applicable isotherm model should be able to account for thermal effects because the gas adsorption processes are nonisothermal. Therefore, in the present work several isotherm models with temperature-dependent parameters were chosen for comparison.

Theory

According to Yang (1987), isotherm models can be categorized by the following three approaches: the Langmuir approach, the Gibbs approach, and the potential theory approach. In the Langmuir approach, experimental ammonia adsorption data are fitted to the Langmuir and Langmuir–Freundlich isotherm equations with five temperature-dependent models. In the present study, the isotherm model is a group of equations that include the actual isotherm equation and equations for the temperature dependence of parameters. The Henry isotherm model and the four vacancy solution (VS) theory isotherm models are treated in the Gibbs approach. In addition to the original form of the VS-Margules model, the extended VS-Margules and VS-Wilson models are derived, since thermodynamically reasonable temperature dependences for the saturation sorbate concentration and the Wilson parameters can be found. In the potential theory approach, the Dubinin–Astakhov isotherm model is considered. This model is improved by using the saturated liquid volumes of the Hankinson–Brobst–Thomson (HBT) equation.

Langmuir approach for isotherm models

Langmuir Isotherm. The minimum number of independent parameters required to fit nonlinear equilibrium data to the isotherm model with a temperature-dependent parameter is three. This is valid for the Langmuir model:

$$q^* = \frac{q_s bp}{1 + bp}. \tag{1}$$

In this model, according to Langmuir's original derivation, the saturation sorbate concentration q_s is temperature-independent and the adsorption equilibrium constant b is temperature-dependent. The physically meaningful temperature dependence of parameter b has been derived from the van't Hoff equation, which relates the parameter b to the limiting heat of adsorption ΔH (Ruthven, 1984):

$$b = b_0 \exp\left(\frac{-\Delta H}{RT}\right). \tag{2}$$

The Langmuir isotherm model, where q_s is temperature-independent and b temperature-dependent according to Eq. 2, will be called the Langmuir 1 model in this work. Table 1 shows the isotherm models that consist of the actual isotherm equation together with the temperature-dependent equations of the isotherm parameters as well as the number of independent parameters in the model.

In many cases, the saturation sorbate concentration has been seen to decrease as the temperature increases. This has been explained by the thermal expansion of sorbate species (Malek and Farooq, 1996). Various temperature-dependent equations have been stated for q_s, but the exact functional form and the thermodynamic consistency of the parameters are not completely validated. Two equations for q_s that have

Table 1. Isotherm Models Studied

Isotherm Model	Eq.	Eq. for Temp. Dependence of Parameters	No. of Independent Parameters
Langmuir 1	1	2	3
Langmuir 2	1	2 and 3	4
Langmuir 3	1	2 and 4	4
Langmuir 4	1	2 and 5	4
Langmuir 5	1	2 and 7	4
Langmuir–Freundlich 1	8	2	4
Langmuir–Freundlich 2	8	2 and 3	5
Langmuir–Freundlich 3	8	2 and 4	5
Langmuir–Freundlich 4	8	2 and 5	5
Langmuir–Freundlich 5	8	2 and 7	5
Henry	9	2	2
VS-Margules 1	10	2	4
VS-Margules 2	10	2 and 7	5
VS-Wilson	11	2, 7, 12 and 13	7
VS-FH	15	2, 15 and 16	5
Dubinin–Astakhov	20	18	3

been used, especially for process simulation models, are (Tsai et al., 1983; Malek and Farooq, 1996; Hwang et al., 1997)

$$q_s = a_1 + \frac{a_2}{T} \tag{3}$$

$$q_s = b_1 \exp\left(\frac{-b_2}{T}\right). \tag{4}$$

Although these equations have not achieved wide acceptance because of a thermodynamic inconsistency, they are tested in this study as Langmuir 2 and 3 models (Table 1).

In addition to these two equations, the temperature dependence of q_s has been expressed (von Gemmingen, 1993; Sievers and Mersmann, 1994) as

$$q_s = q_{s0}\left[1 - \alpha(T - T_0)\right] \tag{5}$$

where q_{s0} is the saturation sorbate concentration at the reference temperature T_0. In Eq. 5, the physical meaning of the parameters is obvious, since q_s is dependent on the thermal expansion coefficient α. Nevertheless, the functional form needs more detailed investigation. By assuming that the saturation sorbate concentration and the volume of liquidlike sorbate are proportional,

$$q_s \propto V_a,$$

and taking into account the decrease of q_s with increasing temperature, the commonly accepted thermal expansion equation (Castellan, 1983) can be converted to the following form:

$$\frac{1}{q_s}\frac{\partial q_s}{\partial T} = -\alpha. \tag{6}$$

Integration of Eq. 6 leads to a different form than Eq. 5:

$$q_s = q_{s0} \exp\left[-\alpha(T - T_0)\right]. \tag{7}$$

Do and coworkers have also presented the same equation form for q_s (Do and Do, 1997; Ahmadpour et al., 1998). The temperature-dependent equations (Eqs. 5 and 7) of q_s were used in the Langmuir 4 and the Langmuir 5 models, respectively (Table 1).

Langmuir−Freundlich Isotherm. The Langmuir−Freundlich isotherm model is popular, since it has the ability to model a wide variety of equilibrium data. It is an explicit equation, which is a significant benefit in process simulation compared to implicit equations, such as vacancy solution theory models. The Langmuir−Freundlich isotherm is generally considered an empirical equation because exponent n has been added to the Langmuir isotherm without a proper physical meaning (Ruthven, 1984; Do, 1998), but the thermodynamic basis of exponent has also been discussed (Rudzinski et al., 1995). Nevertheless, one should notice that Langmuir's theory also contains an equation for dissociative adsorption where the equation has nonunity exponents (Masel, 1996). Therefore, exponent n is included to describe the number of molecules in one adsorption site, that is, it represents the surface heterogeneity. The Langmuir−Freundlich isotherm equation is expressed as

$$q^* = \frac{q_s b p^n}{1 + b p^n}. \tag{8}$$

For the temperature-dependent parameter b, the same equation (Eq. 2) is used as for the Langmuir isotherm models. The Langmuir−Freundlich 1 model does not contain the temperature-dependent q_s, but it is included in the other Langmuir−Freundlich models studied, as with the Langmuir models (Table 1). The parameter n is assumed to be temperature-independent in all models. The number of independent parameters in the Langmuir−Freundlich model equations is four or five.

Gibbs approach for isotherm models

The Gibbs adsorption isotherm is a thermodynamically solid basis to start the derivation of isotherm equations, which provides a general relationship between spreading pressure and adsorbed phase concentration. Any existing equation of state can be chosen for the adsorbed phase. Then several different isotherm equations can be obtained, including the Langmuir, Volmer, van der Waals, and virial isotherms (Ruthven, 1984; Yang, 1987). Here we treat only the Henry and vacancy solution theory isotherm models in this context.

Henry Isotherm. The Henry isotherm model is the simplest model, containing only two independent parameters. It is applicable for linear adsorption data:

$$q^* = Kp, \tag{9}$$

where K is the Henry constant. Its temperature dependence follows the van't Hoff equation in which the preexponential factor and heat of adsorption are K_0 and ΔH, respectively (Ruthven, 1984).

Vacancy Solution Theory. The vacancy solution (VS) theory isotherm model was introduced by Suwanayen and Danner (1980a,b) for the prediction of adsorption equilibria in gas mixtures. It is also suitable for single-component adsorption equilibria. The vacancy means a hypothetical solvent that is thought to occupy the adsorption sites in the sorbent before the access of sorbate species. Single-component adsorption, for example, is treated as a phase-equilibrium between two binary vacancy solutions of different compositions. The nonideality of adsorbed phase has been solved by the use of activity coefficients. Again, the different activity coefficient models produce different isotherm models. The simplest form of the vacancy solution theory isotherm model can be derived by using the two-suffix Margules equation for the activity coefficient:

$$p = \left(\frac{q_s}{b}\frac{\theta}{1-\theta}\right)\exp\left(-\frac{2w_{1v}\theta}{RT}\right), \tag{10}$$

where $\theta = q^*/q_s$.

Two VS-Margules isotherm models were formed in the present study; the VS-Margules 1 model is similar to that presented by Suwanayen and Danner, that is, the parameters w_{1v} and q_s have no temperature dependence. The VS-Margules 2 model is an improvement on the VS-Margules 1 model, because the temperature dependence of Eq. 7 has been added for q_s. Both VS-Margules models obtain the temperature dependence for b from Eq. 2. The VS-Margules 1 and 2 models contain four and five independent parameters, respectively.

If the Wilson equation for the activity coefficient is used, the isotherm equation (Eq. 10) can be written as

$$p = \left(\frac{q_s}{b}\frac{\theta}{1-\theta}\right)\left(\Lambda_{1v}\frac{1-(1-\Lambda_{v1})\theta}{\Lambda_{1v}+(1-\Lambda_{1v})\theta}\right) \exp\left(-\frac{\Lambda_{v1}(1-\Lambda_{v1})\theta}{1-(1-\Lambda_{v1})\theta}-\frac{(1-\Lambda_{1v})\theta}{\Lambda_{1v}+(1-\Lambda_{1v})\theta}\right). \quad (11)$$

The van't Hoff equation (Eq. 2) is valid for the temperature dependence of b in Eq. 11. Suwanayen and Danner did not include a temperature dependence for q_s and Wilson parameters Λ_{1v} and Λ_{v1}. However, the Wilson parameters have thermodynamically consistent temperature-dependent equations (Walas, 1985):

$$\Lambda_{1v} = \frac{V_v^L}{V_1^L}\exp\left(-\frac{\lambda_{1v}}{RT}\right) \quad (12)$$

$$\Lambda_{v1} = \frac{V_1^L}{V_v^L}\exp\left(-\frac{\lambda_{v1}}{RT}\right), \quad (13)$$

which are used in the present work. Here the exponential parameters λ_{1v} and λ_{v1} implicitly describe the surface interaction between sorbate and vacancy. Below the critical temperature, the molar volume of component 1, namely, ammonia, is assumed to be a saturated liquid volume. Following the recommendation of Reid et al. (1987), it can be calculated by the HBT equation. For the vacancy component, it is neither possible nor necessary to calculate the liquid or gas volumes, because they would only be imaginary. The temperature dependence of q_s is shown by Eq. 7. There are seven independent parameters in the VS-Wilson model.

Cochran et al. (1985) introduced the simplified form of Eq. 11, since they found the Wilson parameters to be highly correlated and the original model does not include the effect of temperature. They used a Flory−Huggins-type expression for the activity coefficients, which gives the isotherm equation:

$$p = \left(\frac{q_s}{b}\frac{\theta}{1-\theta}\right)\exp\left(\frac{\alpha_{1v}^2\theta}{1+\alpha_{1v}\theta}\right). \quad (14)$$

The temperature dependence of parameter b follows Eq. 2. For q_s, the following equation was presented:

$$q_s = q_{s0}\exp\left(\frac{r_1}{T}\right), \quad (15)$$

which is an empirical correlation without physical significance. The temperature dependence of α_{1v} is also expressed by an empirical equation:

$$\alpha_{1v} = m_1 q_s - 1. \quad (16)$$

Table 1 shows the four vacancy solution isotherm models studied. At low coverage, the vacancy solution theory isotherm equations reduce to the Langmuir equation.

Potential theory approach for isotherm models

In the potential theory, adsorption is explained as originating as a potential field existing at the sorbent surface. It extends long-range attractive forces on the surrounding gas. Essentially, the potential field decreases as the distance from the surface increases. The potential theory has a unique feature compared to the other isotherm models, namely, the parameters measured at one temperature can be used in the extrapolation of isotherms at other temperatures. Dubinin and his coworkers have modified the original potential theory, for example, by introducing a functional form for a characteristic curve (Reich et al., 1980; Mehta and Danner, 1985; Yang, 1987).

Dubinin− Astakhov Isotherm. According to the potential theory, the volume of a pure sorbate per mass of sorbent W is characterized by an adsorption potential ϵ, which is defined as the work required to remove one mol of sorbate from the surrounding gas to the sorbent surface. The sorbate species inside the sorbent are thought to behave as liquids below critical temperatures (Yang, 1987). The potential theory states that the characteristic curve, that is, W as a function of ϵ, should be temperature-independent for different sorbent−sorbate systems. In the present study, the characteristic curve is not considered, since the aim is to use the potential theory for the modeling of measured adsorption data.

The adsorption potential has the following functional form (Ackley and Yang, 1991):

$$\epsilon = RT\ln\left(\frac{p_s}{p}\right). \quad (17)$$

The sorbate volume W is expressed by the equation

$$W = q^* V_m. \quad (18)$$

Dubinin and Astakhov proposed the following equation for the relationship of W and ϵ (Ackley and Yang, 1991):

$$W = W_0\exp\left[\left(\frac{-\epsilon}{E}\right)^n\right]. \quad (19)$$

If Eq. 19 is expressed analogously to the previous adsorption isotherm equations, it can be rewritten as

$$q^* = \frac{W_0}{V_m}\exp\left[\left(\frac{-\epsilon}{E}\right)^n\right]. \quad (20)$$

The molar volume V_m is assumed to be the same as that of a saturated liquid volume below the critical temperature, where it can be obtained from the HBT equation. The HBT equation is used, since Reich et al. recommend it, although the Rackett equation has been more popular with potential theory models (Mehta and Danner, 1985; Yun et al., 1998). Saturated vapor pressures are calculated by the Antoine equation (Reid et al., 1987), which gives the same results as were measured by Zander and Thomas (1979) for temperatures from 298 to 393 K.

Experimental

Adsorption equilibrium isotherms were measured for 13X zeolite, 4A zeolite, activated alumina, silica gel, and activated carbon sorbents listed in Table 2 at a pressure range of 0–100 kPa and at temperatures of 298, 323, 343 and 393 K. The zeolite and alumina samples were predried overnight at 573 K and silica gel and activated carbon were dried at 473 K prior to measurements. The purity of ammonia gas was 99.999% (AGA, Sweden), and it was used without further purification.

Adsorption equilibrium experiments were performed by a static volumetric method with 4 g of sorbent. The apparatus is shown in Figure 1. The experiments were carried out as follows. After a sample flask was connected to the system, the glass chamber was evacuated to < 0.1 Pa. The sorbent sample was degassed for 1 h by evacuating and heating, after which the sample was cooled to the measuring temperature. The standard volume glass chamber was disconnected from the pumps and the sample flask. The pressure in the chamber was raised with ammonia gas to 1.2–10.0 kPa. The valve to the sample flask was opened, and the pressure decrease was measured until the equilibrium pressure was achieved. Subsequent isotherm points were measured in the same way, by repeating the pressure raising and equilibrating steps. Finally, the amount of ammonia adsorbed could be calculated on the basis of the initial and the equilibrium pressures as well as the temperatures and system volumes.

Parameter Estimation Procedure

Experimental adsorption equilibrium data were fitted to the sixteen different isotherm models described in the previous section. The parameter estimation of the actual isotherm equation and the temperature-dependent equations was carried out simultaneously for the equilibrium data at temperatures of 298, 323, 343 and 393 K.

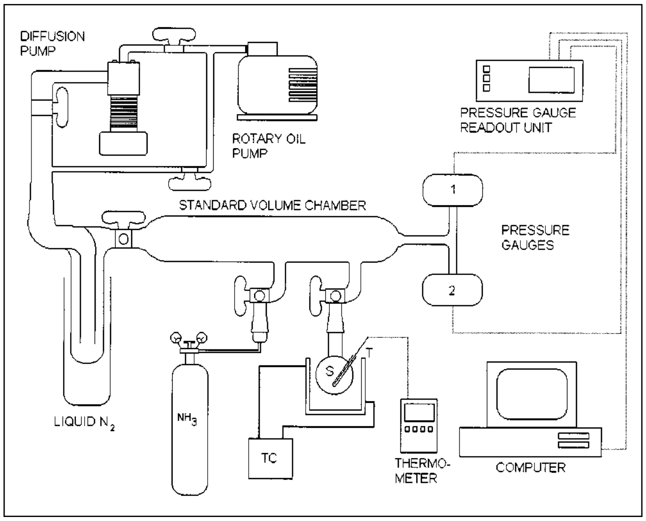

Figure 1. Volumetric adsorption equilibrium apparatus.

Diffusion pump (Leybodiff 40); rotary oil pump (Edwards Speedvac 2); pressure-gauge readout unit (Leybold-Heraeus Inficon CM3); (1) capacitance manometer gauge for 0–1.3332-kPa pressure range (LH Inficon CM100-G10A); (2) capacitance manometer gauge for 0–133.2-kPa pressure range (LH Inficon CM100-G1000A); (T) thermocouple (NiCr-Ni); (TC) temperature-controlled water bath for 298–343 K (Lauda B) and electrically heated mantle for >343 K (Eurotherm thyristor controller); (S) sample flask; and liquid N_2 trap.

The parameters of explicit models were estimated with nonlinear regression by minimizing the weighted sum of residual squares, that is, the differences between the experimental and estimated equilibrium sorbate concentration. The objective function Q to be minimized was expressed as follows:

$$Q = \Sigma w \left(q_p^* - \hat{q}_p^* \right)^2, \tag{21}$$

where p refers to the observed pressures and w is the weight factor. Because the regression with nonequally weighted sorbate concentrations did not give noticeably better results, the weights were given unity. The parameters of implicit models were estimated in the same way, except that during the parameter estimation the unknown coverage θ was solved by a minimization algorithm that combines a golden section search and a successive parabolic interpolation (Brent, 1973). The objective function was therefore minimized by the Levenberg–Marquardt method implemented in the MODEST software (Haario, 1994). At the beginning of each parameter esti-

Table 2. Physical Properties of the Sorbents

Sorbent	Trade Name	Manufacturer	D (mm)	Form	ρ_{bulk} ($\text{kg} \cdot \text{m}^{-3}$)	$a_s^\dagger$ ($\text{m}^2 \cdot \text{g}^{-1}$)	d_{pore} (Å)
13X Zeolite*	Baylith WE894	Bayer	2–3.5	Sphere	647	—	9
4A Zeolite*	Baylith TG242	Bayer	1–1.6	Sphere	778	—	4
Alumina**	LaRoche 1597	LaRoche	2–3	Sphere	735	297	—
Silica gel	Fluka Silica gel 60	—	0.2–0.5	Crushed	445	450	60
AC	Merck Aktivkohle	—	0.5–1	Crushed	436	451	—

*Na form.

**γ-Al_2O_3.

†BET area, measured by N_2 adsorption.

mation procedure, the simplex method was used to search for initial values for the parameters.

In order to enhance the convergence of the minimization procedure, the parameters of the following equations were reparameterized using the mean temperature T_m (Bates and Watts, 1988):

$$b = b_0 \exp\left(\frac{-\Delta H}{R} z\right) \tag{22}$$

$$q_s = a_1 + a_2 z \tag{23}$$

$$q_s = b_1 \exp(-b_2 z) \tag{24}$$

$$p = \left(\frac{q_s}{b}\frac{\theta}{1-\theta}\right)\exp\left(-\frac{2w_{1v}\theta}{R}z\right) \tag{25}$$

$$\Lambda_{1v} = \frac{V_v^L}{V_1^L}\exp\left(-\frac{\lambda_{1v}}{R}z\right) \tag{26}$$

$$\Lambda_{v1} = \frac{V_1^L}{V_v^L}\exp\left(-\frac{\lambda_{v1}}{R}z\right) \tag{27}$$

$$q_s = q_{s0}\exp(r_1 z), \tag{28}$$

where

$$z = \left(\frac{1}{T} - \frac{1}{T_m}\right). \tag{29}$$

In the modeling work, special attention was paid to the correct statistics. Statistical evaluation of the isotherm model accuracy, for example, by the average relative error or the coefficient of determination, is not sufficient. The error of the entire model can be small, although the errors in single parameters are large. If the isotherm model parameters are not statistically reliable and well identifiable, their thermodynamic consistency is also questionable. The extrapolation process scale-up, for example, can be carried out with confidence only if the model is both thermodynamically consistent and its parameters are statistically accurate and reliable. Therefore, the estimated parameters of all isotherm models were evaluated by established statistical methods (Froment and Bischoff, 1990; see also Rönnback et al., 1994; Lehtonen et al., 1995; Toppinen et al., 1996, 1997). The accuracy of fit was evaluated on the basis of several standard statistical values, including the coefficient of determination (R^2), the residual sum of squares (RSS), and the standard error of estimate. The statistical reliability of the estimated parameters was considered using confidence intervals, correlation coefficients, and sensitivity plots.

Results and Discussion

Equilibria and isosteric heats

Figures 2 and 3 show the experimental ammonia adsorption isotherms on 13X zeolite, 4A zeolite, alumina, silica gel, and activated carbon. The ammonia adsorption behavior of 13X and 4A zeolite is very similar: the isotherm forms are highly favorable for adsorption, and ammonia capacities are the same order of magnitude (Figure 2). For example, at a temperature of 298 K, the 13X zeolite has a capacity of 9.33 mmol·g^{-1} at 93.8 kPa, whereas for the 4A zeolite the corresponding value is 8.72 mmol·g^{-1} at 97.8 kPa. The high favor-

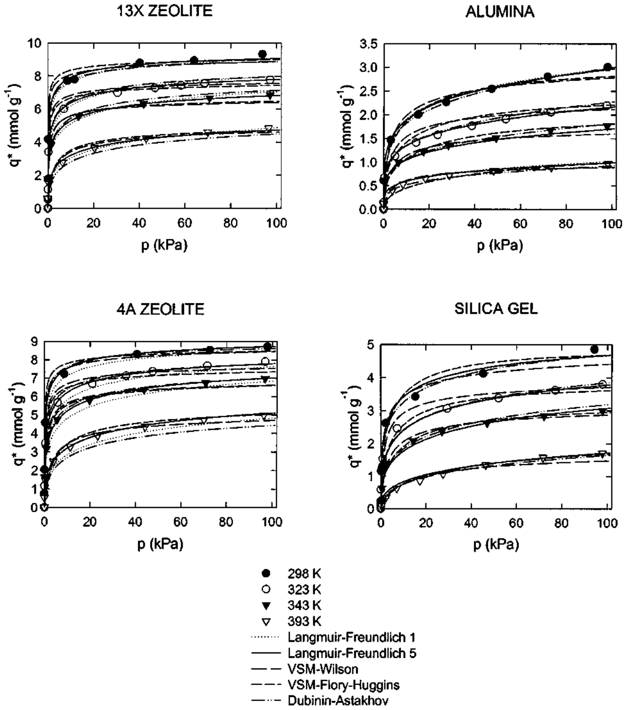

Figure 2. Experimental and predicted ammonia sorbate concentrations at equilibrium on 13X zeolite, 4A zeolite, alumina, and silica gel.

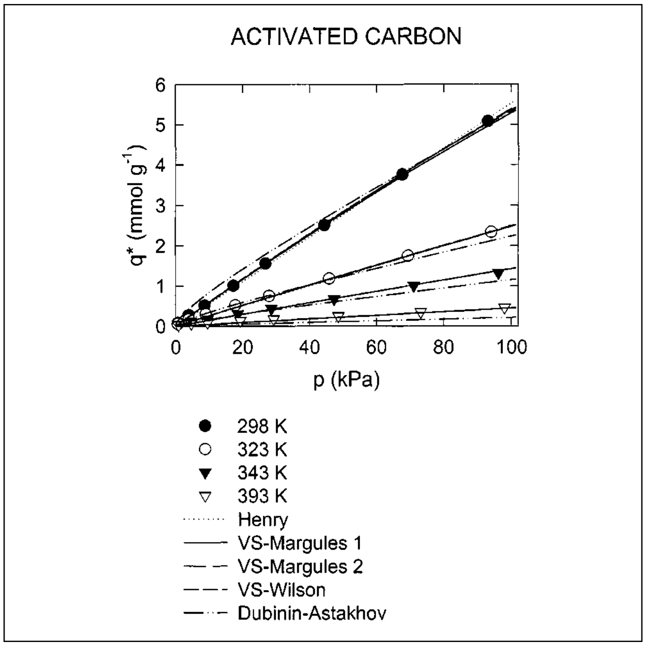

Figure 3. Experimental and predicted ammonia sorbate concentrations at equilibrium on activated carbon.

ableness of isotherms means that the adsorption is nearly irreversible, which decreases the amounts of feasible desorbed ammonia in regeneration by depressurizing. The two zeolites achieve a saturation level at very low pressures, implying that the intracrystalline micropores become filled. After that level, the sorbate concentration continues to rise modestly, corresponding to filling a macroporous binder volume. Alumina and silica gel (Figure 2) do not have as favorable isotherms as the zeolites, but the difference is small. However, these sorbents are not as close to full saturation sorbate concentration as the zeolites because the sorbate concentration increases more rapidly at high pressures. This is a result of the wide distribution of micropore size (Ruthven, 1984). Alumina provides a capacity of 3.01 $mmol \cdot g^{-1}$ at a pressure of 98.3 kPa, which is only 30% of zeolite values at the same temperature.

Correspondingly, silica gel has a higher capacity (4.85 $mmol \cdot g^{-1}$ at 94.3 kPa) than alumina. Ruthven (1984) has presented water adsorption isotherms on 4A zeolite, alumina, and silica gel. If we compare these to the ammonia isotherms of the present work, the similarity of water and ammonia isotherms is clear. This is not surprising, since the properties of ammonia, such as polarity and strong hydrogen bonding tendency, are similar to water (Greenwood and Earnshaw, 1985; Cotton and Wilkinson, 1988). The adsorption isotherm of ammonia on activated carbon (Figure 3) differs completely from the inorganic sorbents over the entire experimental temperature and pressure range, since the isotherm form of activated carbon is linear. At 93 kPa and 298 K, the capacity is fairly high, 5.08 $mmol \cdot g^{-1}$. This is higher than the capacity obtained by Boki et al. (1987) for a standard activated carbon.

The adsorption behavior of ammonia depicted earlier by the isotherms can be considered in more detail by the isosteric heat of adsorption, which is presented in Figure 4. This isosteric heat has been calculated with the Clausius–Clapeyron equation at 298 and 323 K, but the values were also the same at other temperatures. Since the isosteric heat of activated carbon is constant as the sorbate concentration increases, the criteria of a totally homogeneous surface are fulfilled. The isosteric heat of adsorption for activated carbon is also lower than that for the inorganic sorbents. Activated carbon has an isosteric heat of 25.4 $kJ \cdot mol^{-1}$, which reveals relatively weak interactions between the surface and ammonia. The inorganic sorbents create much stronger bonds with ammonia. Surprisingly, the isosteric heats of adsorption are almost the same at 1 $mmol \cdot g^{-1}$ for all inorganic sorbents. Silica gel has the highest value (53.0 $kJ \cdot mol^{-1}$), and the two zeolites have the lowest isosteric heat (47.2 $mmol \cdot g^{-1}$ for 4A zeolite). The previously reported high values of isosteric heat of adsorption for the 4A zeolite at low coverages (Ruthven, 1984; Zhdanov et al., 1990) could not be measured in this work because the equilibrium pressures were lower than the gauge accuracy. The increase in isosteric heat of adsorption with the sorbate concentration implies that intermolecular attractions are stronger than the effect of energetic heterogeneity. Consequently, the surface heterogeneity of inorganic sorbents at the measured sorbate concentration range is not predominant. The heterogeneity would occur as sorbate–cation interactions at the sorbate concentrations lower than 0.9 $mmol \cdot g^{-1}$, since in the sodium form the 13X and 4A zeolites have 10–12 cations in a cage (Ruthven, 1984). The isosteric heat of adsorption for zeolites begins to rise rapidly at 6 $mmol \cdot g^{-1}$, which means a proximity to full saturation.

The preliminary selection of sorbent, for example, for the PSA process, is complicated as the result of adsorption equilibrium isotherms at several temperatures. Here this problem is solved by comparing the capacity difference at pressures of 1 and 100 kPa, that is, the working capacity as a function of temperature for all sorbents in one plot. This comparison is valid only when the selectivity is high, as when ammonia is separated from ammonia–air mixtures. The results are illustrated in Figure 5. It can be seen that activated carbon provides the highest working capacity at 298 K, namely, 5.5 $mmol \cdot g^{-1}$, which drops rapidly to its lowest level at 393 K. Activated carbon would be an ideal sorbent for processes

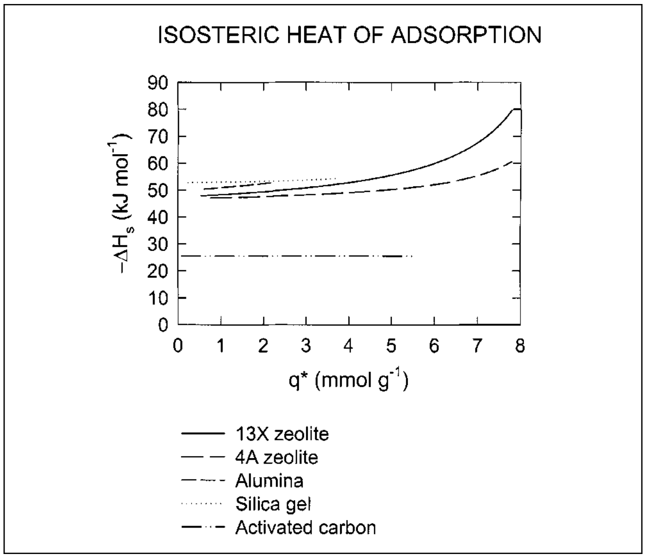

Figure 4. Isosteric heats of adsorption for ammonia.

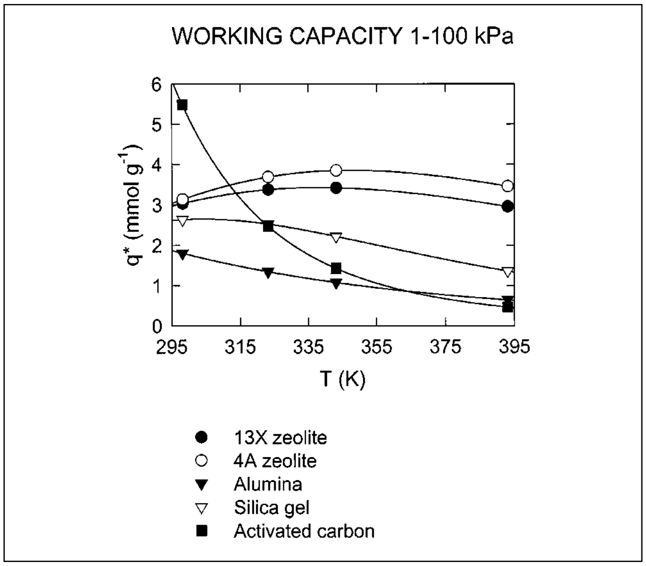

Figure 5. Working capacities in the adsorption of ammonia with the pressure range of 1–100 kPa.

where a high-concentration feed at 298 K is available. The zeolites are very temperature insensitive. In practice, they have almost the same working capacity, 3.0–3.5 $\text{mmol}\cdot\text{g}^{-1}$, over the entire temperature range. That makes them suitable for the PSA process with the feed at high temperatures. Silica gel and alumina do not show good working capacities at any of the studied temperatures.

Table 3. Estimated Parameter Values of the Langmuir and the Langmuir–Freundlich Models for the 13X Zeolite Sorbent

Isotherm Model	Isotherm Parameters	R^2, %	Total SS	RSS	Std. Err. of Estimate
Langmuir 1	$q_s = 7.51 \pm 0.26\ \text{mmol}\cdot\text{g}^{-1}$ $b_0 = 0.735 \pm 0.166\ \text{kPa}^{-1}$ $-\Delta H = 63.3 \pm 5.0\ \text{kJ}\cdot\text{mol}^{-1}$	92.08	289	23.0	0.890
Langmuir 2	$a_1 = 6.63 \pm 0.17\ \text{mmol}\cdot\text{g}^{-1}$ $a_2 = 4{,}920 \pm 594\ \text{mmol}\cdot\text{K}\cdot\text{g}^{-1}$ $b_0 = 1.57 \pm 0.34\ \text{kPa}^{-1}$ $-\Delta H = 36.8 \pm 5.9\ \text{kJ}\cdot\text{mol}^{-1}$	96.68	289	9.6	0.590
Langmuir 3	$b_1 = 6.51 \pm 0.19\ \text{mmol}\cdot\text{g}^{-1}$ $-b_2 = 727 \pm 97\ \text{K}$ $b_0 = 1.49 \pm 0.31\ \text{kPa}^{-1}$ $-\Delta H = 38.4 \pm 5.5\ \text{kJ}\cdot\text{mol}^{-1}$	96.71	289	9.5	0.580
Langmuir 4	$q_{s0} = 10.9 \pm 0.5\ \text{mmol}\cdot\text{g}^{-1}$ $\alpha = 3.80 \pm 0.32 \times 10^{-3}\ \text{K}^{-1}$ $b_0 = 1.58 \pm 0.36\ \text{kPa}^{-1}$ $-\Delta H = 36.7 \pm 6.2\ \text{kJ}\cdot\text{mol}^{-1}$	96.47	289	10.2	0.604
Langmuir 5	$q_{s0} = 12.7 \pm 0.9\ \text{mmol}\cdot\text{g}^{-1}$ $\alpha = 6.57 \pm 0.87 \times 10^{-3}\ \text{K}^{-1}$ $b_0 = 1.58 \pm 0.34\ \text{kPa}^{-1}$ $-\Delta H = 36.7 \pm 5.8\ \text{kJ}\cdot\text{mol}^{-1}$	96.69	289	9.6	0.585
Langmuir–Freundlich 1	$q_s = 10.8 \pm 0.5\ \text{mmol}\cdot\text{g}^{-1}$ $b_0 = 0.454 \pm 0.037\ \text{kPa}^{-1}$ $-\Delta H = 18.7 \pm 1.4\ \text{kJ}\cdot\text{mol}^{-1}$ $n = 0.325 \pm 0.018$	99.46	289	1.6	0.240
Langmuir–Freundlich 2	$a_1 = 8.70 \pm 0.40\ \text{mmol}\cdot\text{g}^{-1}$ $a_2 = 3{,}490 \pm 633\ \text{mmol}\cdot\text{K}\cdot\text{g}^{-1}$ $b_0 = 0.691 \pm 0.072\ \text{kPa}^{-1}$ $-\Delta H = 16.0 \pm 1.7\ \text{kJ}\cdot\text{mol}^{-1}$ $n = 0.387 \pm 0.022$	99.67	289	0.95	0.190
Langmuir–Freundlich 3	$b_1 = 8.78 \pm 0.41\ \text{mmol}\cdot\text{g}^{-1}$ $-b_2 = 361 \pm 75\ \text{K}$ $b_0 = 0.668 \pm 0.067\ \text{kPa}^{-1}$ $-\Delta H = 16.5 \pm 1.5\ \text{kJ}\cdot\text{mol}^{-1}$ $n = 0.382 \pm 0.022$	99.67	289	0.94	0.190
Langmuir–Freundlich 4	$q_{s0} = 12.0 \pm 0.5\ \text{mmol}\cdot\text{g}^{-1}$ $\alpha = 2.53 \pm 0.47 \times 10^{-3}\ \text{K}^{-1}$ $b_0 = 0.668 \pm 0.075\ \text{kPa}^{-1}$ $-\Delta H = 15.3 \pm 2.0\ \text{kJ}\cdot\text{mol}^{-1}$ $n = 0.377 \pm 0.022$	99.64	289	1.1	0.198
Langmuir–Freundlich 5	$q_{s0} = 12.5 \pm 0.6\ \text{mmol}\cdot\text{g}^{-1}$ $\alpha = 3.65 \pm 0.74 \times 10^{-3}\ \text{K}^{-1}$ $b_0 = 0.697 \pm 0.073\ \text{kPa}^{-1}$ $-\Delta H = 15.4 \pm 1.7\ \text{kJ}\cdot\text{mol}^{-1}$ $n = 0.386 \pm 0.023$	99.66	289	0.97	0.190

Table 4. Estimated Parameter Values of the Vacancy Solution and the Dubinin–Astakhov Models for the 13X Zeolite Sorbent

Isotherm Model	Isotherm Parameters	R^2, %	Total SS	RSS	Std. Err. of Estimate
VS-Margules 1	$b_0 = 5.46 \pm 1.27\ \text{kPa}^{-1}$ $-\Delta H = 62.5 \pm 6.5\ \text{kJ}\cdot\text{mol}^{-1}$ $q_s = 7.51 \pm 0.27\ \text{mmol}\cdot\text{g}^{-1}$ $-w_{1v} = 0.67 \pm 2.46\ \text{kJ}\cdot\text{mol}^{-1}$	92.11	289	22.8	0.903
VS-Margules 2	$b_0 = 10.7 \pm 2.3\ \text{kPa}^{-1}$ $-\Delta H = 31.7 \pm 18.0\ \text{kJ}\cdot\text{mol}^{-1}$ $q_{s0} = 12.5 \pm 1.1\ \text{mmol}\cdot\text{g}^{-1}$ $\alpha = 6.41 \pm 1.04 \times 10^{-3}\ \text{K}^{-1}$ $-w_{1v} = 9.8 \pm 16.6\ \text{kJ}\cdot\text{mol}^{-1}$	96.64	289	9.7	0.601
VS-Wilson	$b_0 = 22.7 \pm 5.1\ \text{kPa}^{-1}$ $-\Delta H = 47.3 \pm 7.2\ \text{kJ}\cdot\text{mol}^{-1}$ $q_{s0} = 16.2 \pm 1.6\ \text{mmol}\cdot\text{g}^{-1}$ $\alpha = 6.88 \pm 1.15 \times 10^{-3}\ \text{K}^{-1}$ $-\lambda_{1v} = 110 \pm 33\ \text{kJ}\cdot\text{mol}^{-1}$ $-\lambda_{v1} = 161 \pm 35\ \text{kJ}\cdot\text{mol}^{-1}$ $V_v^L = 78 \pm 111\ \text{dm}^3\cdot\text{mol}^{-1}$	98.21	289	5.2	0.455
VS-FH	$b_0 = 19.2 \pm 3.7\ \text{kPa}^{-1}$ $-\Delta H = 42.6 \pm 5.2\ \text{kJ}\cdot\text{mol}^{-1}$ $q_{s0} = 7.99 \pm 0.34\ \text{mmol}\cdot\text{g}^{-1}$ $r_1 = 588 \pm 94\ \text{K}^{-1}$ $m_1 = 4.3 \pm 2.5 \times 10^{-3}\ \text{g}\cdot\text{mmol}^{-1}$	98.12	289	5.5	0.449
Dubinin-Astakhov	$W_0 = 262 \pm 7 \times 10^{-3}\ \text{cm}^3\cdot\text{g}^{-1}$ $E = 24.8 \pm 0.5\ \text{kJ}\cdot\text{mol}^{-1}$ $n = 2.26 \pm 0.17$	99.08	289	2.7	0.304

Model discrimination

Statistical data presented in Tables 3–11 for all sixteen different isotherm models studied were used for the discrimination and preliminary selection of the models with most potential in ammonia adsorption on 13X zeolite, 4A zeolite, alumina, silica gel, and activated carbon. Langmuir isotherm models fail to correlate the ammonia adsorption equilibrium data on the zeolite, alumina, and silica gel sorbents, as can be seen in Tables 3, 5, 7 and 9. The actual isotherm equation contains only two parameters, which evidently is not enough to describe ammonia adsorption equilibria. Moreover, the Langmuir model does not take into account nonidealities, such as intermolecular attractions and surface heterogeneity, whose contribution is substantial in the adsorption of ammonia on inorganic sorbents. For example, the Langmuir 1 models with temperature-independent q_s have R^2 values of 89.5–92.7%. The introduction of temperature-dependent q_s to the Langmuir models slightly improves the fit. In these models (Langmuir 2–5), the R^2 values vary between 94.1 and 96.7%. Figure 6 shows the fit of Langmuir 1–5 models on the 4A zeolite sorbent. Because the fit of the Langmuir isotherm equation is poor, the accuracy of the temperature-dependent q_s equations cannot be reasonably compared.

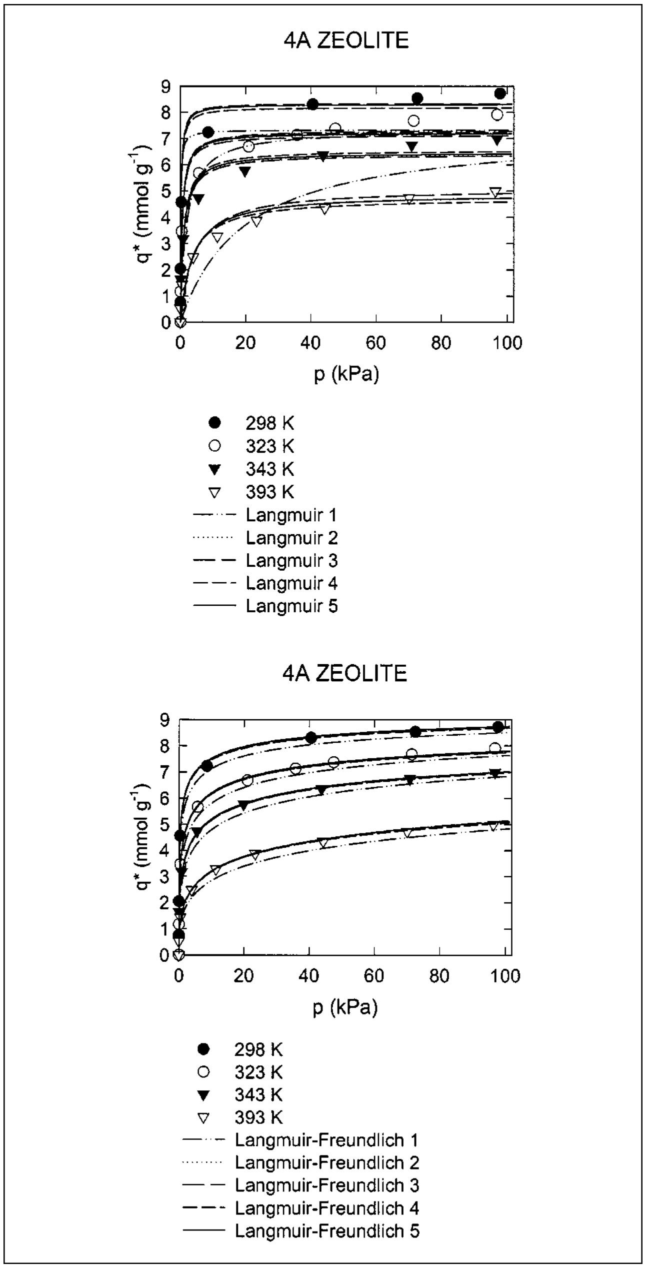

Figure 6. Experimental and predicted ammonia sorbate concentrations at equilibrium on the 4A zeolite sorbent.

Table 5. Estimated Parameter Values of the Langmuir and the Langmuir–Freundlich Models for the 4A Zeolite Sorbent

Isotherm Model	Isotherm Parameters	R^2, %	Total SS	RSS	Std. Err. of Estimate
Langmuir 1	$q_s = 7.33 \pm 0.25$ mmol·g^{-1} $b_0 = 0.650 \pm 0.144$ kPa^{-1} $-\Delta H = 52.5 \pm 5.0$ kJ·mol^{-1}	92.69	269	19.6	0.823
Langmuir 2	$a_1 = 6.58 \pm 0.19$ mmol·g^{-1} $a_2 = 4{,}230 \pm 650$ mmol·K·g^{-1} $b_0 = 1.11 \pm 0.22$ kPa^{-1} $-\Delta H = 28.7 \pm 5.7$ kJ·mol^{-1}	96.14	269	10.4	0.609
Langmuir 3	$b_1 = 6.52 \pm 0.21$ mmol·g^{-1} $-b_2 = 607 \pm 107$ K $b_0 = 1.06 \pm 0.21$ kPa^{-1} $-\Delta H = 30.7 \pm 5.4$ kJ·mol^{-1}	96.02	269	10.7	0.618
Langmuir 4	$q_{s0} = 10.3 \pm 0.5$ mmol·g^{-1} $\alpha = 3.52 \pm 0.37 \times 10^{-3}$ K^{-1} $b_0 = 1.13 \pm 0.23$ kPa^{-1} $-\Delta H = 28.2 \pm 5.8$ kJ·mol^{-1}	96.14	269	10.4	0.608
Langmuir 5	$q_{s0} = 11.5 \pm 0.9$ mmol·g^{-1} $\alpha = 5.57 \pm 0.95 \times 10^{-3}$ K^{-1} $b_0 = 1.11 \pm 0.22$ kPa^{-1} $-\Delta H = 28.9 \pm 5.6$ kJ·mol^{-1}	96.14	269	10.4	0.608
Langmuir–Freundlich 1	$q_s = 9.88 \pm 0.20$ mmol·g^{-1} $b_0 = 0.492 \pm 0.019$ kPa^{-1} $-\Delta H = 19.1 \pm 0.7$ kJ·mol^{-1} $n = 0.375 \pm 0.011$	99.83	269	0.45	0.127
Langmuir–Freundlich 2	$a_1 = 9.19 \pm 0.28$ mmol·g^{-1} $a_2 = 1{,}340 \pm 479$ mmol·K·g^{-1} $b_0 = 0.558 \pm 0.032$ kPa^{-1} $-\Delta H = 18.0 \pm 0.9$ kJ·mol^{-1} $n = 0.397 \pm 0.014$	99.86	269	0.38	0.118
Langmuir–Freundlich 3	$b_1 = 9.25 \pm 0.29$ mmol·g^{-1} $-b_2 = 129 \pm 53$ K $b_0 = 0.551 \pm 0.031$ kPa^{-1} $-\Delta H = 18.2 \pm 0.8$ kJ·mol^{-1} $n = 0.395 \pm 0.014$	99.86	269	0.38	0.119
Langmuir–Freundlich 4	$q_{s0} = 10.6 \pm 0.3$ mmol·g^{-1} $\alpha = 1.47 \pm 0.37 \times 10^{-3}$ K^{-1} $b_0 = 0.578 \pm 0.033$ kPa^{-1} $-\Delta H = 17.1 \pm 1.0$ kJ·mol^{-1} $n = 0.401 \pm 0.013$	99.87	269	0.34	0.113
Langmuir–Freundlich 5	$q_{s0} = 10.7 \pm 0.3$ mmol·g^{-1} $\alpha = 1.57 \pm 0.50 \times 10^{-3}$ K^{-1} $b_0 = 0.571 \pm 0.032$ kPa^{-1} $-\Delta H = 17.5 \pm 0.9$ kJ·mol^{-1} $n = 0.400 \pm 0.014$	99.87	269	0.35	0.114

Tables 3, 5, 7, and 9 show the regression results for all the Langmuir–Freundlich models of zeolite, alumina, and silica gel sorbents. As previously with the Langmuir models, there was no attempt to fit the linear data of activated carbon to the nonlinear Langmuir–Freundlich model. Based on the R^2 values, the Langmuir–Freundlich models provide an extremely accurate fit to the ammonia adsorption data at all measured temperatures. The R^2 values of 13X and 4A zeolite vary between 99.46% and 99.67% and between 99.83% and 99.87%, respectively. The alumina sorbent also has high R^2 values, but the R^2 values of silica gel remain below 98.8%. Since the 4A zeolite data provided the most accurate fit with the Langmuir–Freundlich models, and these isotherms are closer to full saturation than the isotherms of silica gel and alumina, the 4A zeolite data were used to compare the five different approaches to model the saturation sorbate concentration q_s. These results are shown in Figure 6 and Table 5. It can be seen in Figure 6 that the Langmuir–Freundlich 1

Table 6. Estimated Parameter Values of the Vacancy Solution and the Dubinin–Astakhov Models for the 4A Zeolite Sorbent

Isotherm Model	Isotherm Parameters	R^2, %	Total SS	RSS	Std. Err. of Estimate
VS-Margules 1					
	$b_0 = 4.78 \pm 1.05$ kPa^{-1}	92.72	269	19.7	0.836
	$-\Delta H = 51.9 \pm 5.7$ kJ·mol^{-1}				
	$q_s = 7.33 \pm 0.26$ mmol·g^{-1}				
	$-w_{1v} = 0.44 \pm 1.66$ kJ·mol^{-1}				
VS-Margules 2					
	$b_0 = 7.18 \pm 1.35$ kPa^{-1}	96.12	269	10.4	0.622
	$-\Delta H = 33.1 \pm 5.4$ kJ·mol^{-1}				
	$q_{s0} = 11.5 \pm 1.0$ mmol·g^{-1}				
	$\alpha = 5.60 \pm 1.07 \times 10^{-3}$ K^{-1}				
	$-w_{1v} = 0.98 \pm 2.08$ kJ·mol^{-1}				
VS-Wilson					
	$b_0 = 15.5 \pm 2.8$ kPa^{-1}	98.30	269	4.6	0.428
	$-\Delta H = 40.3 \pm 5.6$ kJ·mol^{-1}				
	$q_{s0} = 14.1 \pm 1.2$ mmol·g^{-1}				
	$\alpha = 5.31 \pm 0.95 \times 10^{-3}$ K^{-1}				
	$-\lambda_{1v} = 1.45 \pm 1.11$ kJ·mol^{-1}				
	$-\lambda_{v1} = 74.0 \pm 16.3$ kJ·mol^{-1}				
	$V_v^L = 1.10 \pm 0.85$ dm^3·mol^{-1}				
VS-FH					
	$b_0 = 12.8 \pm 1.8$ kPa^{-1}	98.02	269	5.3	0.444
	$-\Delta H = 42.9 \pm 3.5$ kJ·mol^{-1}				
	$q_{s0} = 8.50 \pm 0.20$ mmol·g^{-1}				
	$r_1 = 407 \pm 34$ K^{-1}				
	$m_1 = 0.556 \pm 0.533 \times 10^{-3}$ g·mmol^{-1}				
Dubinin-Astakhov					
	$W_0 = 252 \pm 6 \times 10^{-3}$ cm^3·g^{-1}	98.96	269	2.8	0.310
	$E = 24.6 \pm 0.5$ kJ·mol^{-1}				
	$n = 2.47 \pm 0.18$				

Table 7. Estimated Parameter Values of the Langmuir and the Langmuir–Freundlich Models for the Alumina Sorbent

Isotherm Model	Isotherm Parameters	R^2, %	Total SS	RSS	Std. Err. of Estimate
Langmuir 1					
	$q_s = 2.51 \pm 0.14$ mmol·g^{-1}	89.51	24	2.5	0.290
	$b_0 = 0.0590 \pm 0.0135$ kPa^{-1}				
	$-\Delta H = 39.0 \pm 5.0$ kJ·mol^{-1}				
Langmuir 2					
	$a_1 = 1.85 \pm 0.09$ mmol·g^{-1}	94.55	24	1.3	0.220
	$a_2 = 2{,}280 \pm 276$ mmol·K·g^{-1}				
	$b_0 = 0.197 \pm 0.058$ kPa^{-1}				
	$-\Delta H = 6.55 \pm 7.82$ kJ·mol^{-1}				
Langmuir 3					
	$b_1 = 1.74 \pm 0.11$ mmol·g^{-1}	94.45	24	1.3	0.220
	$-b_2 = 1{,}210 \pm 180$ K				
	$b_0 = 0.195 \pm 0.056$ kPa^{-1}				
	$-\Delta H = 7.24 \pm 7.40$ kJ·mol^{-1}				
Langmuir 4					
	$q_{s0} = 3.80 \pm 0.25$ mmol·g^{-1}	94.07	24	1.4	0.200
	$\alpha = 4.91 \pm 0.39 \times 10^{-3}$ K^{-1}				
	$b_0 = 0.178 \pm 0.052$ kPa^{-1}				
	$-\Delta H = 9.73 \pm 8.02$ kJ·mol^{-1}				
Langmuir 5					
	$q_{s0} = 5.51 \pm 0.71$ mmol·g^{-1}	94.67	24	1.3	0.214
	$\alpha = 11.4 \pm 1.7 \times 10^{-3}$ K^{-1}				
	$b_0 = 0.209 \pm 0.062$ kPa^{-1}				
	$-\Delta H = 4.77 \pm 7.84$ kJ·mol^{-1}				
Langmuir–Freundlich 1					
	$q_s = 11.7 \pm 3.9$ mmol·g^{-1}	99.68	24	0.08	0.052
	$b_0 = 0.0588 \pm 0.0204$ kPa^{-1}				
	$-\Delta H = 13.1 \pm 0.8$ kJ·mol^{-1}				
	$n = 0.243 \pm 0.014$				
Langmuir–Freundlich 2					
	$a_1 = 10.8 \pm 5.4$ mmol·g^{-1}	99.79	24	0.05	0.043
	$a_2 = 9{,}690 \pm 4{,}980$ mmol·K·g^{-1}				
	$b_0 = 0.0668 \pm 0.0351$ kPa^{-1}				
	$-\Delta H = 4.64 \pm 1.04$ kJ·mol^{-1}				
	$n = 0.240 \pm 0.017$				
Langmuir–Freundlich 3					
	$b_1 = 11.6 \pm 9.0$ mmol·g^{-1}	99.66	24	0.08	0.055
	$-b_2 = 222 \pm 820$ K				
	$b_0 = 0.0505 \pm 0.0483$ kPa^{-1}				
	$-\Delta H = 10.9 \pm 7.1$ kJ·mol^{-1}				
	$n = 0.241 \pm 0.022$				
Langmuir–Freundlich 4					
	$q_{s0} = 13.6 \pm 4.7$ mmol·g^{-1}	99.78	24	0.05	0.044
	$\alpha = 3.37 \pm 0.41 \times 10^{-3}$ K^{-1}				
	$b_0 = 0.0796 \pm 0.0279$ kPa^{-1}				
	$-\Delta H = 7.95 \pm 1.31$ kJ·mol^{-1}				
	$n = 0.249 \pm 0.016$				
Langmuir–Freundlich 5					
	$q_{s0} = 15.2 \pm 7.4$ mmol·g^{-1}	99.73	24	0.07	0.049
	$\alpha = 4.11 \pm 3.84 \times 10^{-3}$ K^{-1}				
	$b_0 = 0.0695 \pm 0.0302$ kPa^{-1}				
	$-\Delta H = 8.81 \pm 4.16$ kJ·mol^{-1}				
	$n = 0.244 \pm 0.017$				

model with temperature-independent q_s is incapable of accurately predicting the ammonia sorbate concentrations. The differences between the Langmuir–Freundlich 2–5 models are smaller than the experimental error. The Langmuir–Freundlich 4 and 5 models have precisely the same R^2 value, 99.87%. However, the Langmuir–Freundlich 4 model has somewhat lower RSS and the standard error of estimate values, which means that the Langmuir–Freundlich 4 model provides a better fit. In practice, the difference is insignificant and both models give as accurate results. As discussed in the theory section, the temperature dependence equation of the Langmuir–Freundlich 5 model appears to have the most reasonable thermodynamic basis. Therefore, we use it with the VS-Margules 2 and VS-Wilson models.

The fits of Langmuir–Freundlich models are accurate on the inorganic sorbents. However, the accuracy of fit is not an exclusively satisfactory criterion, but the errors of the Langmuir–Freundlich model parameters also need further consideration (Tables 3, 5, 7, and 9). It can be seen that the errors of the Langmuir–Freundlich 1–5 models for 4A zeolite are of the same size and very small compared to the other inorganic sorbents. For alumina, the magnitude of errors between the Langmuir–Freundlich 1–5 models is different. For example, the errors of $-\Delta H$ are 16.4–64.8% for the Langmuir–Freundlich 2–5 models and only 6.2% for the Langmuir–Freundlich 1 model. The large errors are the result of the poor identifiability of $-\Delta H$ in the Langmuir–Freundlich 2–5 models. This can be explained by the one additional parameter for the saturation sorbate concentration compared to the Langmuir–Freundlich 1 model, which could not be reliably determined due to the lack of saturation data on alumina. The poor identifiability can also be observed in the

Table 8. Estimated Parameter Values of the Vacancy Solution and the Dubinin–Astakhov Models for the Alumina Sorbent

Isotherm Model	Isotherm Parameters	R^2, %	Total SS	RSS	Std. Err. of Estimate
VS-Margules 1					
	$b_0 = 0.147 \pm 0.028$ kPa^{-1}	89.71	24	2.5	0.297
	$-\Delta H = 35.3 \pm 9.9$ kJ·mol^{-1}				
	$q_s = 2.50 \pm 0.14$ mmol·g^{-1}				
	$-w_{1v} = 3.7 \pm 10.9$ kJ·mol^{-1}				
VS-Margules 2					
	$b_0 = 0.333 \pm 0.084$ kPa^{-1}	94.58	24	1.3	0.220
	$-\Delta H = 17.4 \pm 6.8$ kJ·mol^{-1}				
	$q_{s0} = 5.17 \pm 0.77$ mmol·g^{-1}				
	$\alpha = 10.6 \pm 1.9 \times 10^{-3}$ K^{-1}				
	$-w_{1v} = 0.68 \pm 1.39$ kJ·mol^{-1}				
VS-Wilson					
	$b_0 = 0.699 \pm 0.244$ kPa^{-1}	96.07	24	0.94	0.194
	$-\Delta H = 17.7 \pm 11.6$ kJ·mol^{-1}				
	$q_{s0} = 9.43 \pm 1.87$ mmol·g^{-1}				
	$\alpha = 14.0 \pm 2.6 \times 10^{-3}$ K^{-1}				
	$-\lambda_{1v} = 49.1 \pm 38.4$ kJ·mol^{-1}				
	$-\lambda_{v1} = 95.6 \pm 35.2$ kJ·mol^{-1}				
	$V_v^L = 3.37 \pm 5.05$ dm^3·mol^{-1}				
VS-FH					
	$b_0 = 52.5 \pm 6.4$ kPa^{-1}	98.43	24	0.38	0.118
	$-\Delta H = 85.6 \pm 7.6$ kJ·mol^{-1}				
	$q_{s0} = 2.15 \pm 0.14$ mmol·g^{-1}				
	$r_1 = 905 \pm 194$ K^{-1}				
	$m_1 = 3.66 \pm 0.16$ g·mmol^{-1}				
Dubinin-Astakhov					
	$W_0 = 0.159 \pm 0.012$ cm^3·g^{-1}	99.78	24	0.05	0.042
	$E = 10.0 \pm 0.9$ kJ·mol^{-1}				
	$n = 0.844 \pm 0.055$				

large errors of the q_s parameters as well as the b parameters. Similar results also are obtained for silica gel. Consequently, for the studied inorganic sorbents, the most reliable values of $-\Delta H$ can be estimated by the Langmuir–Freundlich 1 model. This model is therefore included in the following comparison with the Langmuir–Freundlich 5 models, the VS models, and the Dubinin–Astakhov model.

Tables 4, 6, 8, and 10 show the regression results of VS and Dubinin–Astakhov models on the zeolite, alumina, and silica gel sorbents. The VS-Margules 1 model provides as unsatisfactory a fit as the Langmuir 1 model on inorganic sorbents. In practice, one additional parameter $-w_{1v}$ improves the fit only 0.03% measured as the R^2 value. This is unexpected, because $-w_{1v}$ takes into account the intermolecular attractions (Ruthven, 1984), which are significant on inorganic sorbents. The original model form was improved by introducing a temperature-dependence equation for q_s. This VS-Margules 2 model has R^2 values of 94.6–96.6% for the zeolite, alumina, and silica gel sorbents, which is not acceptable. The VS-Margules models were thus left out of further investigation with the inorganic sorbents. These VS-Margules 1 and 2 models correlate very accurately, however, with the linear ammonia adsorption data on activated carbon (Table 11).

The extended VS-Wilson model, when compared to the original model of Suwanayen and Danner (1980a,b), seems to fit the ammonia adsorption data on the inorganic sorbents relatively well (Tables 4, 6, 8, and 10). It also provides an accurate fit to the equilibrium data of activated carbon (Table 11). Therefore, this model is considered in the final comparison section. The VS-Flory-Huggins model predicts the ammonia equilibria on zeolites, alumina, and silica gel at different temperatures slightly better than the VS-Wilson model.

Table 9. Estimated Parameter Values of the Langmuir and the Langmuir–Freundlich Models for the Silica Gel Sorbent

Isotherm Model	Isotherm Parameters	R^2, %	Total SS	RSS	Std. Err. of Estimate
Langmuir 1					
	$q_s = 3.83 \pm 0.18$ mmol·g^{-1}	92.50	62	4.6	0.400
	$b_0 = 0.108 \pm 0.021$ kPa^{-1}				
	$-\Delta H = 47.9 \pm 4.0$ kJ·mol^{-1}				
Langmuir 2					
	$a_1 = 3.06 \pm 0.13$ mmol·g^{-1}	95.55	62	2.8	0.314
	$a_2 = 3{,}230 \pm 444$ mmol·K·g^{-1}				
	$b_0 = 0.259 \pm 0.064$ kPa^{-1}				
	$-\Delta H = 22.5 \pm 6.4$ kJ·mol^{-1}				
Langmuir 3					
	$b_1 = 3.10 \pm 0.17$ mmol·g^{-1}	95.12	62	3.0	0.329
	$-b_2 = 844 \pm 178$ K				
	$b_0 = 0.204 \pm 0.046$ kPa^{-1}				
	$-\Delta H = 29.2 \pm 5.7$ kJ·mol^{-1}				
Langmuir 4					
	$q_{s0} = 5.88 \pm 0.35$ mmol·g^{-1}	95.59	62	2.7	0.312
	$\alpha = 4.67 \pm 0.38 \times 10^{-3}$ K^{-1}				
	$b_0 = 0.262 \pm 0.065$ kPa^{-1}				
	$-\Delta H = 22.6 \pm 6.5$ kJ·mol^{-1}				
Langmuir 5					
	$q_{s0} = 7.22 \pm 0.90$ mmol·g^{-1}	95.43	62	2.8	0.318
	$\alpha = 8.58 \pm 1.58 \times 10^{-3}$ K^{-1}				
	$b_0 = 0.235 \pm 0.0552$ kPa^{-1}				
	$-\Delta H = 25.2 \pm 6.0$ kJ·mol^{-1}				
Langmuir–Freundlich 1					
	$q_s = 6.21 \pm 0.61$ mmol·g^{-1}	98.72	62	0.79	0.168
	$b_0 = 0.172 \pm 0.018$ kPa^{-1}				
	$-\Delta H = 21.2 \pm 1.9$ kJ·mol^{-1}				
	$n = 0.396 \pm 0.032$				
Langmuir–Freundlich 2					
	$a_1 = 6.05 \pm 1.31$ mmol·g^{-1}	98.71	62	0.80	0.172
	$a_2 = 348 \pm 2{,}000$ mmol·K·g^{-1}				
	$b_0 = 0.177 \pm 0.043$ kPa^{-1}				
	$-\Delta H = 20.8 \pm 3.2$ kJ·mol^{-1}				
	$n = 0.400 \pm 0.047$				
Langmuir–Freundlich 3					
	$b_1 = 5.92 \pm 1.22$ mmol·g^{-1}	98.69	62	0.81	0.173
	$-b_2 = 107 \pm 314$ K				
	$b_0 = 0.181 \pm 0.042$ kPa^{-1}				
	$-\Delta H = 20.5 \pm 3.1$ kJ·mol^{-1}				
	$n = 0.404 \pm 0.047$				
Langmuir–Freundlich 4					
	$q_{s0} = 6.41 \pm 1.28$ mmol·g^{-1}	98.72	62	0.79	0.171
	$\alpha = 0.691 \pm 3.66 \times 10^{-3}$ K^{-1}				
	$b_0 = 0.181 \pm 0.053$ kPa^{-1}				
	$-\Delta H = 20.5 \pm 4.7$ kJ·mol^{-1}				
	$n = 0.402 \pm 0.048$				
Langmuir–Freundlich 5					
	$q_{s0} = 6.37 \pm 1.31$ mmol·g^{-1}	98.72	62	0.79	0.171
	$\alpha = 0.516 \pm 4.02 \times 10^{-3}$ K^{-1}				
	$b_0 = 0.178 \pm 0.051$ kPa^{-1}				
	$-\Delta H = 20.7 \pm 4.4$ kJ·mol^{-1}				
	$n = 0.400 \pm 0.049$				

The VS-Flory-Huggins model fails to predict the ammonia equilibria on activated carbon, so the model is only used with the inorganic sorbents.

The Dubinin−Astakhov model correlates well with both the adsorption data of the inorganic sorbents and the activated carbon. The R^2 value ranges from 98.96% to 99.78% for the zeolites, alumina, and silica gel. The quality of fitting is also satisfactory in the case of activated carbon, that is, the R^2 value is 98.84%. These results show that the Dubinin−Astakhov model is useful for ammonia adsorption and is worth more detailed investigation.

Final comparison of isotherm models

The statistical data presented in Tables 3−11 do not give enough information for the comparison of the models, for example, how well the models predict the saturation sorbate concentration or at which temperature the model prediction fails. This information can only be obtained by comparing the isotherm plots where the predicted and measured values are presented. Figure 2 shows the comparison of the Langmuir−Freundlich 1 model, the Langmuir−Freundlich 5 model, the VS-Wilson model, the VS-Flory-Huggins model, and the Dubinin−Astakhov model for the ammonia adsorption equilibria on 13X zeolite, 4A zeolite, alumina, and silica gel. The Langmuir−Freundlich 5 model provides the most accurate fit on the 13X zeolite data. This model is capable of predicting the ammonia sorbate concentrations at the entire temperature and pressure range. The Langmuir−Freundlich 1 model fails in predicting high-pressure concentrations. The VS-Wilson and VS-Flory-Huggins models correlate similarly with the ammonia equilibrium data: the prediction fails both at low and high pressures. These models do not satisfactorily depict the ammonia equilibria. The Dubinin−Astakhov model behaves differently. It predicts quite precisely the ammonia sorbate concentrations at 298 and 323 K, but fails at 343 and 393 K.

Table 10. Estimated Parameter Values of the Vacancy Solution and the Dubinin–Astakhov Models for the Silica Gel Sorbent

Isotherm Model	Isotherm Parameters	R^2, %	Total SS	RSS	Std. Err. of Estimate
VS-Margules 1					
	$b_0 = 0.413 \pm 0.030$ kPa^{-1}	92.50	62	4.6	0.407
	$-\Delta H = 47.9 \pm 3.6$ kJ·mol^{-1}				
	$q_s = 3.83 \pm 0.15$ mmol·g^{-1}				
	$-w_{1v} = 0.073 \pm 0.274$ kJ·mol^{-1}				
VS-Margules 2					
	$b_0 = 0.700 \pm 0.151$ kPa^{-1}	95.30	62	2.9	0.328
	$-\Delta H = 31.9 \pm 6.0$ kJ·mol^{-1}				
	$q_{s0} = 7.31 \pm 1.11$ mmol·g^{-1}				
	$\alpha = 8.72 \pm 1.85 \times 10^{-3}$ K^{-1}				
	$-w_{1v} = 0.691 \pm 1.65$ kJ·mol^{-1}				
VS-Wilson					
	$b_0 = 1.42 \pm 0.28$ kPa^{-1}	97.74	62	1.4	0.237
	$-\Delta H = 42.9 \pm 6.6$ kJ·mol^{-1}				
	$q_{s0} = 11.6 \pm 2.0$ mmol·g^{-1}				
	$\alpha = 10.3 \pm 2.0 \times 10^{-3}$ K^{-1}				
	$-\lambda_{1v} = 8.3 \pm 15.5$ kJ·mol^{-1}				
	$-\lambda_{v1} = 121 \pm 36$ kJ·mol^{-1}				
	$V_v^L = 6.1 \pm 10.5$ dm^3·mol^{-1}				
VS-FH					
	$b_0 = 22.1 \pm 14.1$ kPa^{-1}	98.64	62	0.88	0.177
	$-\Delta H = 76.5 \pm 7.2$ kJ·mol^{-1}				
	$q_{s0} = 3.34 \pm 0.16$ mmol·g^{-1}				
	$r_1 = 962 \pm 143$ K^{-1}				
	$m_1 = 1.80 \pm 0.20$ g·mmol^{-1}				
Dubinin-Astakhov					
	$W_0 = 159 \pm 10 \times 10^{-3}$ cm^3·g^{-1}	98.97	62	0.63	0.148
	$E = 16.7 \pm 0.8$ kJ·mol^{-1}				
	$n = 1.62 \pm 0.15$				

Table 11. Estimated Parameter Values of the Henry Model, the Vacancy Solution Models, and the Dubinin–Astakhov Model for the Activated Carbon Sorbent

Isotherm Model	Isotherm Parameters	R^2, %	Total SS	RSS	Std. Err. of Estimate
Henry					
	$K_0 = 15.9 \pm 0.2 \times 10^{-3}$ mmol·g^{-1}	99.86	44	0.06	0.042
	$-\Delta H = 25.4 \pm 0.3$ kJ·mol^{-1}				
VS-Margules 1					
	$b_0 = 16.3 \pm 0.2 \times 10^{-3}$ kPa^{-1}	99.92	44	0.04	0.034
	$-\Delta H = 26.4 \pm 0.3$ kJ·mol^{-1}				
	$q_s = 47.2 \pm 7.2$ mmol·g^{-1}				
	$-w_{1v} = 1.92 \pm 0.71$ kJ·mol^{-1}				
VS-Margules 2					
	$b_0 = 18.0 \pm 0.5 \times 10^{-3}$ kPa^{-1}	99.93	44	0.03	0.032
	$-\Delta H = 23.9 \pm 0.8$ kJ·mol^{-1}				
	$q_{s0} = 33.2 \pm 5.6$ mmol·g^{-1}				
	$\alpha = 11.3 \pm 2.5 \times 10^{-3}$ K^{-1}				
	$-w_{1v} = 9.90 \pm 0.72$ kJ·mol^{-1}				
VS-Wilson					
	$b_0 = 16.3 \pm 0.2 \times 10^{-3}$ kPa^{-1}	99.91	44	0.04	0.037
	$-\Delta H = 26.8 \pm 0.4$ kJ·mol^{-1}				
	$q_{s0} = 96.3 \pm 23.1$ mmol·g^{-1}				
	$\alpha = 0.944 \pm 0.568 \times 10^{-3}$ K^{-1}				
	$-\lambda_{1v} = 31.3 \pm$ large kJ·mol^{-1}				
	$-\lambda_{v1} = 2.91 \pm$ large kJ·mol^{-1}				
	$V_v^L = 0.336 \pm 0.252$ dm^3·mol^{-1}				
VS-FH					
	$b_0 = 34 \pm 142$ kPa^{-1}	75.54	44	10.8	0.589
	$-\Delta H = 86.5 \pm 32.1$ kJ·mol^{-1}				
	$q_{s0} = 5.07 \pm 9.31$ mmol·g^{-1}				
	$r_1 = 73 \pm 233$ K^{-1}				
	$m_1 = 2.41 \pm 3.96$ g·mmol^{-1}				
Dubinin-Astakhov					
	$W_0 = 2.31 \pm 2.06$ cm^3·g^{-1}	98.84	44	0.51	0.125
	$E = 1.51 \pm 1.15$ kJ·mol^{-1}				
	$n = 0.751 \pm 0.187$				

The Langmuir−Freundlich 5 model gives the best fit on the ammonia equilibrium data on 4A zeolite (Figure 2). The model works almost perfectly covering all measured temperatures and pressures. As discussed earlier, the Langmuir−Freundlich 1 model fails in the prediction of the saturation sorbate concentrations because the saturation sorbate parameter is temperature-independent. The VS-Wilson model and the VS-Flory-Huggins model are not successful in predicting the ammonia equilibria on 4A zeolite. They cannot predict the increasing sorbate concentration as pressure increases, but remain at the constant saturation sorbate concentration level, similar to the Langmuir models. The Dubinin−Astakhov model correlates accurately at 298, 323, and 343 K. However, it fails at a temperature of 393 K.

Interestingly, the Langmuir–Freundlich 1 model is as accurate as the Langmuir–Freundlich 5 model on alumina. They show exactly the same curve in Figure 2. This means that the temperature-dependent q_s is not necessarily needed at pressures of 0–100 kPa, since the full saturation level is at a considerably higher pressure. The VS-Wilson and VS-Flory-Huggins models also fail with the alumina sorbent. The Dubinin–Astakhov model provides the best fit on alumina. It reliably predicts the ammonia equilibria at all measured pressures and temperatures.

As earlier with alumina, the Langmuir–Freundlich 1 and 5 models provide a similar fit on silica gel. The reason is also the same as with alumina. Generally, the fit is very accurate. The VS-Wilson and VS-Flory-Huggins models do not give a satisfactory fit on silica gel, as was observed with other inorganic sorbents. The VS-Wilson model should be able to describe the intermolecular attractions in the bulk phase and adsorbed phase as well as the attractions between sorbate and the sorbent, that is, the surface heterogeneity (Suwanayen and Danner, 1980a,b). Because the fits are not accurate, though all important nonidealities are considered in the VS-Wilson model, implicitly embedding nonidealities in the activity coefficient is apparently not correct in the case of adsorption of ammonia. The Dubinin–Astakhov model predicts reliably the ammonia equilibria on silica gel. The fit is more accurate than with the Langmuir–Freundlich models.

In practice, the Henry model, VS-Margules 1 model, the VS-Margules 2 model, and the VS-Wilson model similarly predict the ammonia adsorption on activated carbon (Figure 3). The Dubinin–Astakhov model fails, especially at temperatures of 323, 343, and 393 K. At these temperatures the Dubinin–Astakhov model systematically underpredicts sorbate concentrations. The low-pressure range causes overpredictions at 298 and 323 K.

Finally, besides the standard deviations presented in Tables 3–11, the estimated parameters were statistically evaluated by the calculation of correlation coefficients and sensitivities. The correlation coefficients were generally high for almost all models, which is quite typical with multiparametric models. For example, the correlation coefficients of parameters α and q_{s0} as well as α and b_0 were higher than 0.8 for the Langmuir–Freundlich 5 model with the 4A zeolite sorbent. Altogether six parameter pairs had a correlation coefficient higher than 0.5. The correlation coefficients, however, do not give information about the identifiability and reliability of the parameters. As mentioned earlier, Cochran et al. (1985) have noticed that the parameters of the VS-Wilson model are highly correlated. Based on the present results, the correlation coefficients of the VS-Wilson model are not high, for example, the number of parameter pairs higher than 0.5 is only four for the 4A zeolite data. Therefore, we have not included the correlation matrices in the results. Consequently, the identifiability of the estimated model parameters has been compared using sensitivity plots, where the coefficient of determination R^2 is presented as a function of one parameter, keeping the other parameters at their optimum values. Figures 7 and 8 show the identifiability of parameters as an example for the Langmuir–Freundlich 5 and VS-Wilson models, respectively. It can be noticed from Figure 7 that the R^2 value has a sharp optimum with all parameters in the Langmuir–Freundlich 5 model. This implies that the parameters are well identified and thus statistically reliable. The parameters of the VS-Wilson model have problems with identifiability, for example, for the 4A zeolite data, the parameters q_{s0}, α, and $-\Delta H$ have a sharp optimum, but the parameters b_0, $-\lambda_{v1}$, and V_V^L have only a one-sided identification (Figure 8). The parameter $-\lambda_v$ is generally poorly identified. As a result, the parameters of the VS-Wilson model could not reliably be statistically determined and thus be considered physically meaningful. In this study, the lack of parameter identifiability is valid for all models with more than five parameters.

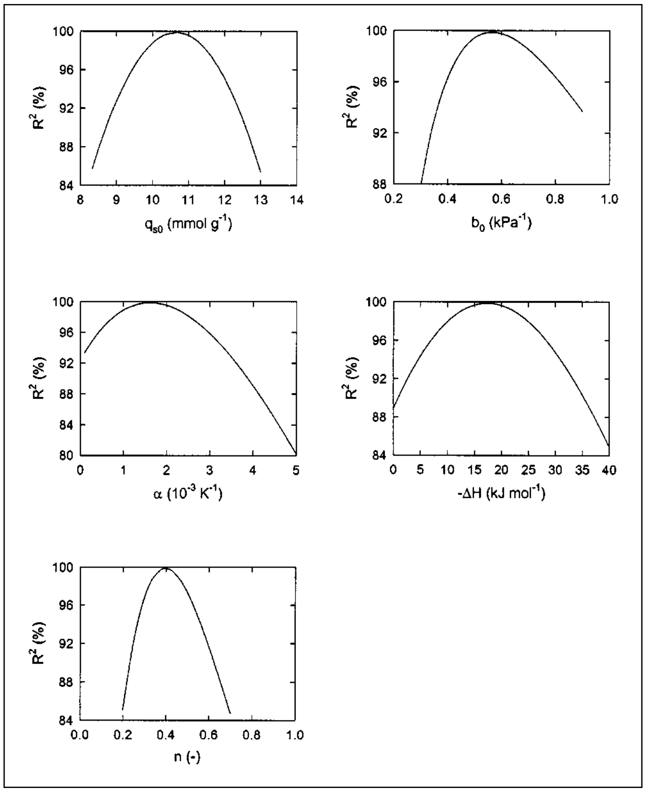

Figure 7. Coefficient of determination as a function of the Langmuir–Freundlich 5 parameter values for the 4A zeolite.

Conclusions

Ammonia gas adsorption experiments on 13X zeolite, 4A zeolite, alumina, silica gel, and activated-carbon sorbents were carried out at temperatures between 298 and 393 K and at pressures below 100 kPa. Under these conditions, ammonia adsorbed most strongly on the 13X and 4A zeolites. These sorbents have the highest ammonia capacity. Unfortunately, the form of the adsorption isotherms is highly favorable for adsorption, and regeneration by depressurizing is difficult. The isotherms of silica gel and alumina are also favorable, but not as favorable as those of the zeolites. The difference is small, however, and the capacity remains considerably lower than that of the zeolites. The adsorption of ammonia is completely different on activated carbon and on inorganic sorbents. The isotherms are linear, and thus the capacity is poor at low pressures.

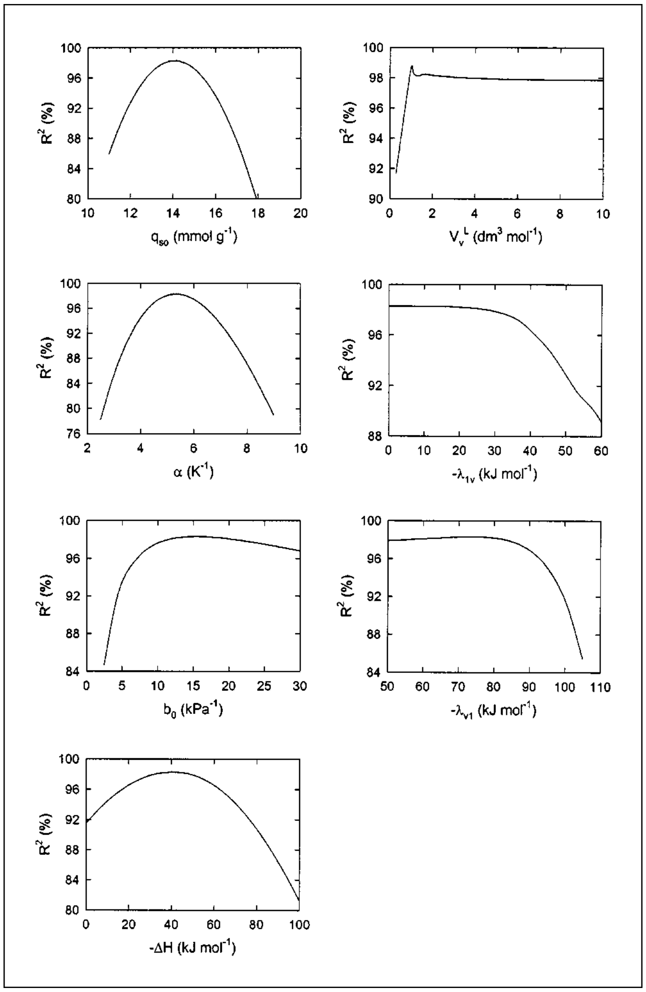

Figure 8. Coefficient of determination as a function of the VS-Wilson parameter values for the 4A zeolite.

Interesting features were revealed in the comparison of the applicability of the zeolites, alumina, silica gel, and activated carbon based on working capacities between 1 and 100 kPa. For example, activated carbon has the highest working capacity, approximately 5.5 mmol·g^{-1}, at 298 K. However, it decreases rapidly with temperature, reaching its lowest level at 393 K. Activated carbon would be a rational choice at 298 K for an industrial ammonia PSA sorbent, when other components are nonadsorbing and the ammonia concentration in the feed is high. The 13X and 4A zeolites are insensitive to temperature since they have almost the same working capacity over the entire temperature range, namely 3.0–3.5 mmol·g^{-1}. Therefore, the zeolites work best in processes where the feed is hot. Additionally, the zeolites are good at separating ammonia at very low concentrations. Silica gel and alumina are the sorbents that have the lowest working capacity at 298 K. The working capacity drops continuously as the temperature increases. Under the experimental conditions of the present study, alumina and silica gel do not provide any advantages.

For comparison, sixteen different isotherm models were fitted to the experimental data. A large number of models was necessary, since there is no universally applicable isotherm equation for the modeling of adsorption equilibria. The Langmuir models and the vacancy solution models failed with the data from ammonia adsorption on inorganic sorbents. The Langmuir–Freundlich models with a temperature-dependent adsorption equilibrium constant from the van't Hoff equation and with a temperature-dependent saturation sorbate concentration in the thermal expansion equation generally provided the best fit on all inorganic sorbents. This model gave the most accurate prediction of the 13X and 4A zeolite data, but with the alumina and silica gel data, the Dubinin–Astakhov model gave the best fit. The Dubinin–Astakhov model failed in the prediction of equilibria at high temperatures, especially with the zeolite data. The Henry model and the vacancy solutions models, with the exception of the VS-Flory-Huggins model, provide a very accurate fit on activated carbon. The results clearly indicate that the functional form of the isotherm equation has a greater impact on the accuracy of the fit than the number of independent parameters. The functional form of the saturation sorbate concentration equation has a very small effect. Additionally, the large number of independent parameters leads to poor identification when the estimated parameters are not statistically reliable, and thus their physical meaning is also questionable.

Acknowledgment

This work has been carried out in a cooperation with Kemira Chemicals Corporation as a part of NORES project financed by the Technology Development Centre (TEKES). The financial support to Jarkko Helminen from the Kemira Foundation is gratefully acknowledged. We also thank Bayer AG and LaRoche Industries Inc. for supplying the sorbents.

Notation

a_1 = empirical constant for saturation sorbate concentration, mmol·g^{-1}
a_2 = empirical constant for saturation sorbate concentration, mmol·g^{-1}·K
b_0 = preexponential factor, kPa^{-1}
b_1 = empirical constant for saturation sorbate concentration, mmol·g^{-1}
b_2 = empirical constant for saturation sorbate concentration, K
E = characteristic free energy of adsorption, kJ·mol^{-1}
m_1 = empirical constant for saturation sorbate concentration, mmol^{-1}·g
p_s = saturation pressure, kPa
q_p^* = experimental sorbate concentration in equilibrium at pressure p, mmol·g^{-1}
$\hat{q}_p^*$ = predicted sorbate concentration in equilibrium at pressure p, mmol·g^{-1}
R = gas constant, 8.314 J·mol^{-1}·K^{-1}
r_1 = empirical constant for saturation sorbate concentration, K
V_v^L = saturated liquid volume of vacancy, cm^3·mol^{-1}
V_1^L = saturated liquid volume of sorbate, cm^3·mol^{-1}
W_0 = pore volume, cm^3·g^{-1}
w_{1v} = regular solution parameter for surface interaction between sorbate and vacancy, kJ·mol^{-1}
z = transformed temperature, K^{-1}

Literature Cited

Ackley, M. W., and R. T. Yang, "Adsorption Characteristics of High-Exchange Clinoptilolites," *Ind. Eng. Chem. Res.*, **31**, 2523 (1991).

Ahmadpour, A., K. Wang, and D. D. Do, "Comparison of Models on the Prediction of Binary Equilibrium Data of Activated Carbons," *AIChE J.*, **44**, 740 (1998).

Bates, D. M., and D. G. Watts, *Nonlinear Regression Analysis and Its Applications*, Wiley, New York (1988).

Boki, K., S. Tanada, O. Nobuhiro, S. Tsutsui, R. Yamasaki, and M. Nakamura, "Adsorption of Polar and Nonpolar Gases of Different Sizes on Nitrogen-Containing Activated Carbon," *J. Colloid Interface Sci.*, **120**, 286 (1987).

Brent, R. P., *Algorithms for Minimization Without Derivatives*, Prentice Hall, Englewood Cliffs, NJ (1973).

Castellan, G. W., *Physical Chemistry*, Addison-Wesley, Reading, MA (1983).

Chiachotni, K., K. Heden, D. Dushanov, V. Minkova, and D. Ruschev, "Adsorption of Some Gases on Activated Carbon at High Pressure," *Bulg. Acad. Sci.*, **24**, 420 (1991).

Cochran, T. W., R. L. Kabel, and R. P. Danner, "Vacancy Solution Theory of Adsorption Using Flory-Huggins Activity Coefficient Equations, *AIChE J.*, **31**, 268 (1985).

Cotton, F. A., and G. Wilkinson, *Advanced Inorganic Chemistry*, Wiley, New York (1988).

Do, D. D., and Ha. D. Do, "A New Adsorption Isotherm for Heterogeneous Adsorbent Based on the Isosteric Heat as a Function of Loading," *Chem. Eng. Sci.*, **52**, 297 (1997).

Do, D. D., *Adsorption Analysis: Equilibria and Kinetics*, Imperial College Press, London (1998).

Froment, G. F., and K. B. Bischoff, *Chemical Reactor Analysis and Design*, Wiley, New York (1990).

Greenwood, N. N., and A. Earnshaw, *Chemistry of the Elements*, Pergamon, Oxford (1985).

Haario, H., *MODEST Users Manual*, ProfMath Oy, Helsinki (1994).

Hirai, H., M. Komiyama, K. Kurima, and K. Wada, "Adsorbent for Use in Selective Gas Adsorption Separation and a Process for Producing the Same," U.S. Patent No. 4,675,309 (1987).

Hwang, K. S., D. K. Choi, S. Y. Gong, and S. Y. Cho, "Adsorption and Thermal Regeneration of Methylene Chloride Vapor on an Activated Carbon Bed," *Chem. Eng. Sci.*, **52**, 1111 (1997).

Isalski, W. H., "Recovery of Hydrogen and Ammonia from Pure Gas," U.S. Patent No. 4,266,957 (1981).

Knaebel, K. S., "For Your Next Separation Consider Adsorption," *Chem. Eng.*, **102**, 92 (1995).

Knaebel, K. S., "Pressure Swing Adsorption System for Ammonia Synthesis," U.S. Patent No. 5,711,926 (1998).

Kuo, S.-L., E. O. Pedram, and A. L. Hines, "Analysis of Ammonia Adsorption on Silica Gel Using the Modified Potential Theory," *J. Chem. Eng. Data*, **30**, 330 (1985).

Lavie, R., "Process for the Manufacture of Ammonia," U.S. Patent No. 4,537,760 (1985).

Lehtonen, J., T. Salmi, A. Vuori, H. Haario, and P. Nousiainen, "Modeling of the Kinetics of Alkali Fusion," *Ind. Eng. Chem. Res.*, **34**, 3678 (1995).

Malek, A., and S. Farooq, "Comparison of Isotherm Models for Hydrocarbon Adsorption on Activated Carbon," *AIChE J.*, **42**, 3191 (1996).

Masel, R. I., *Principles of Adsorption and Reaction on Solid Surfaces*, Wiley, New York (1996).

Mehta, S. D., and R. P Danner, "An Improved Potential Theory Method for Predicting Gas-Mixture Adsorption Equilibria," *Ind. Eng. Chem. Fundam.*, **24**, 325 (1985).

Reich, R., W. T. Ziegler, and K. A. Rogers, "Adsorption of Methane, Ethane, and Ethylene Gases and Their Binary and Ternary Mixtures and Carbon Dioxide on Activated Carbon at 212−301 K and Pressures to 35 Atmospheres," *Ind. Eng. Chem. Process Des. Dev.*, **19**, 336 (1980).

Reid, R. C., J. M. Prausnitz, and B. E. Poling, *The Properties of Gases & Liquids*, McGraw-Hill, New York (1987).

Rönnback, R., T. Salmi, A. Vuori, H. Haario, J. Lehtonen, A. Sundqvist, and E. Tirronen, "Development of a Kinetic Model for the Esterification of Acetic Acid with Methanol in the Presence of a Homogeneous Acid Catalyst," *Chem. Eng. Sci.*, **52**, 3369 (1997).

Ruthven, D. M., *Principles of Adsorption and Adsorption Processes*, Wiley, New York (1984).

Ruthven, D. M., S. Farooq, and K. S. Knaebel, *Pressure Swing Adsorption*, VCH, New York (1994).

Rudzinski, W., K. Nieszporek, H. Moon, and H.-K. Rhee, "On the Theoretical Origin and Applicability of the Potential Theory Approach to Predict Mixed-Gas Adsorption on Solid Surfaces from Single-Gas Adsorption Isotherms," *Chem. Eng. Sci.*, **50**, 2641 (1995).

Shiralkar, V. P., and S. B. Kulkarni, "Sorption of Ammonia in Cation-Exchanged Y Zeolites: Isotherms and State of Sorbed Molecules," *J. Colloid Interface Sci.*, **108**, 1 (1985).

Sievers, W., and A. Mersmann, "Single and Multicomponent Adsorption Equilibria of Carbon Dioxide, Nitrogen, Carbon Monoxide and Methane in Hydrogen Purification Processes," *Chem. Eng. Technol.*, **17**, 325 (1994).

Spindler, H., D. Pape, H. Preuss, and R. Entner, "Adsorption Equilibrium Measurement of Ammonia at 5A-Molecular Sieves Under Pressure," *Chem. Tech. (Leipzig)*, **42**, 432 (1990).

Suwanayuen, S., and R. P. Danner, "A Gas Adsorption Isotherm Equation Based on Vacancy Solution Theory, *AIChE J.*, **26**, 68 (1980a).

Suwanayuen, S., and R. P. Danner, "Vacancy Solution Theory of Adsorption From Gas Mixtures," *AIChE J.*, **26**, 76 (1980b).

Toppinen, S., T.-K. Rantakylä, T. Salmi, and J. Aittamaa, "Kinetics of Liquid-Phase Hydrogenation of Benzene and Some Monosubstituted Alkylbenzenes over a Nickel Catalyst," *Ind. Eng. Chem. Res.*, **35**, 1824 (1996).

Toppinen, S., T. Salmi, T.-K. Rantakylä, and J. Aittamaa, "Liquid-Phase Hydrogenation Kinetics of Aromatic Hydrocarbon Mixtures," *Ind. Eng. Chem. Res.*, **36**, 2101 (1997).

Tsai, M. C., S. S. Wang, and R. T. Yang, "Pore-Diffusion Model for Cyclic Separation: Temperature Swing Separation of Hydrogen and Methane at Elevated Pressure," *AIChE J.*, **29**, 966 (1983).

Valenzuela, D. P., and A. L. Myers, *Adsorption Equilibrium Data Handbook*, Prentice Hall, Englewood Cliffs, NJ (1989).

von Gemmingen, U., "A New Approach to Adsorption Isotherms," *Gas Sep. Purif.*, **7**, 175 (1993).

Walas, S. M., *Phase Equilibria in Chemical Engineering*, Butterworth, Boston (1985).

Yang, R. T., *Gas Separation by Adsorption Processes*, Butterworth, Boston (1987).

Yun, J. H., D. K. Choi, and S. H. Kim, "Adsorption Equilibria of Chlorinated Organic Solvents onto Activated Carbon," *Ind. Eng. Chem. Res.*, 37, 1422 (1998).

Zander, M., and W. Thomas, "Some Thermodynamic Properties of Liquid Ammonia: PVT Data, Vapor Pressure, and Critical Temperature," *J. Chem. Eng. Data*, **24**, 1 (1979).

Zhdanov, S. P., S. S. Khvoshchev, and N. N. Feoktistova, *Synthetic Zeolites*, Gordon & Breach, New York (1990).

Manuscript received Sept. 20, 1999, and revision received Feb. 18, 2000.